Journal of Operation and Automation in Power Engineering

Vol. 10, No. 1, Apr. 2022, Pages: 80-89

http://joape.uma.ac.ir

An Improved FOC Strategy for Speed Control of Induction Motor Drives Under an Open-Phase Fault Using Genetic Algorithm

M. Shabandokht-Zarami[1], M. Ghanbari[1,], E. Alibeiki[1,2], M. Jannati[1]*

[1]*Department of Electrical Engineering, Gorgan Branch, Islamic Azad University, Gorgan, Iran*

[2]*Department of Electrical Engineering, Aliabad Katoul Branch, Islamic Azad University, Aliabad Katoul, Iran*

Abstract- *The Vector Control (VC) of Y-Connected Induction Motor (YCIM) drives is entirely demanding task. Furthermore, YCIM under an Open-Circuit Fault in the Stator Coils (OCFSC) leads to deterioration of the VC. Consequently, the VC of YCIMs under an OCFSC requires a suitable design. This research focuses on an accurate and modified Field-Oriented Control (FOC) strategy for 3-phase YCIM drives under an OCFSC. Most of the recent papers studying VC of YCIMs under an OCFSC ignore the leakage inductance in the VC equations. This paper presents an alternative VC technique, considering the leakage inductance in the VC equations of YCIMs under an OCFSC. In the presented VC system, two asymmetrical Rotating Transformations (RTs) for the stator current and voltage quantities are proposed and employed. In the proposed scheme, the genetic algorithm is used to regulate the parameters of the Proportional-Integral (PI) controllers. The developed VC system provides an accurate control against an OCFSC and can be employed for different industries that need Fault-Tolerant Control (FTC) systems. The effectiveness of the proposed approach is validated through experimentation in the laboratory. The proposed control scheme gives good responses during both steady state and transient sate. In addition, the proposed VC system gives better performances during the post-fault operation compared to previous works in terms of speed and torque ripples.*

Keyword: Fault-Tolerant Control, Genetic Algorithm, Improved Field-Oriented Control Strategy, Open-Circuit Fault in the Stator Coils, Speed Control of Induction Motor Drives.

NOMENCLATURE

$I_{\alpha s}, I_{\beta s}, I_{\alpha r}, I_{\beta r}$ $V_{\alpha s}, V_{\beta s}, V_{\alpha r}, V_{\beta r}$	Stator and rotor currents and voltages in the $\alpha\beta$ frame (A, V)
I_{as}, I_{bs}, I_{cs}	Stator line currents (A)
$I_{ds}, I_{qs}, I_{dr}, I_{qr}$ $V_{ds}, V_{qs}, V_{dr}, V_{qr}$	Stator and rotor currents and voltages in the dq frame (A, V)
$\Lambda_{\alpha r}, \Lambda_{\beta r}$, $\Lambda_{dr}, \Lambda_{qr}$	Rotor fluxes in the $\alpha\beta$ and dq frames (wb)
r_s, r_r	Stator and rotor resistances (Ω)
l_r, l_m, l_{ls}	Rotor self-inductance, magnetizing inductance, and stator leakage inductance (H)
l_{ds}, l_{qs}, l_d, l_q	Stator dq self and mutual inductances (H)
Ω_r	Rotational speed (rad/s)
T_l, T_e	Load and electromagnetic torques (N.m)
f, j	Viscous friction coefficient and moment of inertia (N.m.s, kg.m^2)
n_p	Number of pole pairs
p	Differential operator
$\lvert\Lambda_r\rvert, \theta_e$	Rotor flux amplitude and angle (wb, rad)
Ω_e	Angular speed of the rotor field-oriented frame (rad/s)
n_d, n_q	dq turn numbers
F	Magneto-Motive Force (MMF) (A)
I_f, V_f	Forward current and forward voltage (A, V)
I_b, V_b	Backward current and backward voltage (A, V)
I_m, V_m	Main current and main voltage (A, V)
I_a, V_a	Auxiliary current and auxiliary voltage (A, V)
k	Turn ratio
T_r	Rotor time constant (H/Ω)
K_p, K_i	Proportional and integral coefficients
Superscripts "f" and "n"	Faulty and normal conditions

Received: 20 Apr. 2021
Revised: 01 May 2021
Accepted: 29 May 2021
∗Corresponding author:
E-mail: ghanbari@gorganiau.ac.ir (M. Ghanbari)
DOI: 10.22098/joape.2022.8721.1608
Research Paper

1. INTRODUCTION

In recent decades, many Y-Connected Induction Motors (YCIMs) are utilized in different industrial drive systems. The typical control strategies for YCIM drives are unreliable in various industries. Hence, Fault-Tolerant Control (FTC) systems are employed instead. The main benefit of these systems is to continue the desired performance of the drive system even in the presence of fault(s) [1, 2]. Generally, FTC systems include two main parts: fault detection and identification mechanisms and post-fault control technique.

In terms of used components in YCIM drives, various faults occur such as power switch faults [2, 3], motor faults [4-6], current sensor faults [7, 8], speed sensor and voltage sensor faults [9], etc. Open-Circuit Fault in the Stator Coils (OCFSC) is one of the most common types of faults which occur in the motor. This fault happens in YCIM drives because of loose connections, power switch failures, rupture of windings, etc. There are various techniques in the literature to control 3-phase IMs under an OCFSC: open-loop scalar control methods [10, 11], closed-loop scalar control methods [12], direct Vector Control (VC) strategies [13, 14], and indirect VC strategies [4-6, 15-19]. These strategies can be divided into two types:

1) The first method is Magneto-Motive Force (MMF)-based control strategies. In Refs. [11, 12], open-loop and closed-loop scalar control methods were proposed for Δ-connected IMs under an OCFSC, respectively. The advantages of scalar control methods include low cost and low hardware complexity. However, the scalar control strategies cannot provide precise speed control features over a wide speed range. Hence, VC or Field-Oriented Control (FOC) techniques are used instead. In Ref. [4], a VC method based on the MMF of the faulty IM was proposed for Δ-connected IMs under an OCFSC. This control method also is not an accurate control strategy during normal condition because of existence of the backward components in the proposed scheme. In Ref. [15], a VC technique was proposed for YCIMs under an OCFSC. The presented control method in Ref. [15] is not suitable during load situations because of using the hysteresis current controller.

2) The second method is the Rotating Transformation (RT)-based control strategies. In Ref. [19], an indirect VC method by the typical RT was proposed for YCIMs under an OCFSC. The presented indirect VC method in Ref. [19] is very difficult to implement due to using two VC systems. In Ref. [5], an indirect VC method with optimal rotor flux based on a current control system was proposed for YCIMs under an OCFSC. This control method is not an accurate control approach during load situations because of using current controller. In Ref. [16], speed senorless VC methods, in Refs. [17, 18] two indirect VC methods, and in Refs. [13, 14] two direct VC methods were proposed for YCIMs under an OCFSC. However, these strategies are not considered as precise VC systems due to the leakage inductance elimination in the VC equations [6]. In Ref. [6], an accurate indirect VC strategy using two unequal RTs was proposed for YCIM drives under an OCFSC. Nevertheless, this approach suffers from derivative components in the VC equations. In addition, the presented indirect VC strategy in Ref. [6] used many Proportional-Integral (PI) controllers.

Accurate determination of the PI controller parameters plays an important role in the drive system performance. The optimization of PI controllers for electric motor drives has always been a hot topic. In Ref. [20], a particle swarm optimization technique was used to regulate the PI controller parameters in the FOC of IM drives. In Ref. [21], a quantum-behaved lightening search system was developed to increase the performance of the FOC fuzzy-PI controller in IM drives. Paper [22] deals with the optimization of fuzzy logic speed controller for DC drives using elastic joints. In Ref. [23], a rotational dq current control system was proposed using the particle swarm optimization for IM drives through an ultra-sparse z-source matrix converter. In Ref. [24], a Luo converter for switched reluctance motors with the particle swarm optimization to tune the parameters of PI controllers was proposed and implemented. Recently, evolutionary algorithms have been favored for tuning PI parameters. Genetic algorithm is one of the most common types of evolutionary algorithms. Genetic algorithm has been regularly utilized in many industrial applications [25-28]. Paper [25] showed that the original steady-state genetic algorithms can hillclimb faster than mutation-only evolutionary systems. In Ref. [26], a hybrid optimization method using genetic algorithm and exchange market algorithm was proposed. In Ref. [27], a hybrid genetic algorithm using the moving least square was use for the optimal design of an axially symmetric dual reflector antenna. In Ref. [28], a cluster-based genetic algorithm with non-dominated elitist selection to support multi-objective test optimization was presented. This research uses a genetic algorithm to optimize PI controllers to improve performance of introduced VC strategy for YCIM drive under OCFSC.

This research proposes an indirect VC system for 3-phase YCIM drives under an OCFSC. In the proposed approach, two RTs are presented and used. Based on these RTs, the VC of the faulty YCIM drive is performed with minor changes in the typical VC scheme. In the proposed VC system the genetic algorithm is utilized to regulate the parameters of PI controllers. To confirm the validity of the proposed control scheme different tests are performed in the laboratory. The achieved results confirm the open-phase fault-tolerant capability of the proposed VC method for YCIM drives. The main contributions of this paper, compared to previous studies, are:

- A modified VC technique with genetic algorithm is proposed for 3-phase YCIM drives under an OCFSC.
- Unlike Refs. [5, 13, 15], the proposed VC technique is appropriate for high power industries due to use of a voltage controller.
- Unlike the previous papers such as Refs. [14, 16-18] that ignore the leakage inductance in the VC model, this parameter is taken into account. In other words, the proposed VC method in this study has better performances compared to Refs. [14, 16-18] in terms of speed and torque ripples.
- Unlike Ref. [6], the proposed VC technique has simple structure due to using fewer PI controllers.

The proposed FOC method in this paper can be employed for many industrial applications such as electric vehicles, aerospace, and military industries which need open-phase FTC systems. In this paper experimental results are given to show the performance of the presented FOC system. Experimental results confirm the claimed FOC structure.

2. PROPOSED VC DESIGN

The YCIM mathematical model under an OCFSC in the $\alpha\beta$ frame is similar to an Asymmetrical Two-Phase Induction Motor (ATPIM) model [14]. Accordingly, the YCIM under an OCFSC is equivalent to an ATPIM as displayed in Fig. 1.

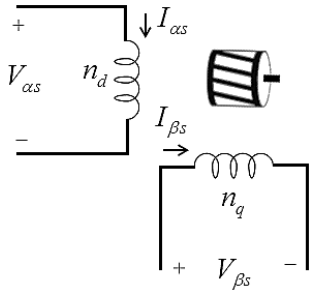

Fig. 1. Asymmetrical Two-Phase Induction Motor (ATPIM)

In this section, two asymmetrical RTs for the stator current and voltage quantities are presented and employed in order to control the YCIM drive under an OCFSC. A current RT is achieved based on the MMF value of the faulty YCIM. Then, a voltage RT is obtained based on the ATPIM model. Afterwards, based on the presented RTs the VC equations are presented. Finally, based on the VC equations and the inverter configuration, the proposed improved VC scheme is shown.

2.1. Current RT

The dq MMFs created by the YCIM during normal condition in the dq frame can be expressed by Eqns. (1) and (2):

$$F_{ds}^{n} = F_{\alpha s}^{n}\cos\theta_e + F_{\beta s}^{n}\sin\theta_e \tag{1}$$

$$F_{qs}^{n} = -F_{\alpha s}^{n}\sin\theta_e + F_{\beta s}^{n}\cos\theta_e \tag{2}$$

Since the YCIM under an OCFSC is equivalent to an ATPIM, the $\alpha\beta$ MMFs created by the faulty YCIM are written as Eqns. (3) and (4):

$$F_{\alpha s}^{f} = n_d I_{\alpha s} \tag{3}$$

$$F_{\beta s}^{f} = n_q I_{\beta s} \tag{4}$$

In order to control the faulty YCIM, the MMF value of the healthy YCIM and the faulty YCIM should be the same [15]. It means:

$$F_{\alpha s}^{n} = F_{\alpha s}^{f} \tag{5}$$

$$F_{\beta s}^{n} = F_{\beta s}^{f} \tag{6}$$

Accordingly, Eqns. (1) and (2) can be expressed by Eqns. (7) and (8):

$$F_{ds}^{n} = n_d I_{\alpha s}\cos\theta_e + n_q I_{\beta s}\sin\theta_e \tag{7}$$

$$F_{qs}^{n} = -n_d I_{\alpha s}\sin\theta_e + n_q I_{\beta s}\cos\theta_e \tag{8}$$

$$\frac{n_d}{n_q} = \frac{l_d}{l_q} \tag{9}$$

$$F_{ds}^{n} = n_q I_{ds} \tag{10}$$

$$F_{qs}^{n} = n_q I_{qs} \tag{11}$$

Eqns. (7) and (8) are written as Eqns. (12) and (13):

$$I_{ds} = \frac{l_d}{l_q} I_{\alpha s}\cos\theta_e + I_{\beta s}\sin\theta_e \tag{12}$$

$$I_{qs} = -\frac{l_d}{l_q} I_{\alpha s}\sin\theta_e + I_{\beta s}\cos\theta_e \tag{13}$$

Accordingly, the current RT is achieved as Eq. (14):

$$\begin{bmatrix} I_{ds} \\ I_{qs} \end{bmatrix} = \begin{bmatrix} T_I \end{bmatrix} \begin{bmatrix} I_{\alpha s} \\ I_{\beta s} \end{bmatrix} = \begin{bmatrix} \frac{l_d}{l_q}\cos\theta_e & \sin\theta_e \\ -\frac{l_d}{l_q}\sin\theta_e & \cos\theta_e \end{bmatrix} \begin{bmatrix} I_{\alpha s} \\ I_{\beta s} \end{bmatrix} \tag{14}$$

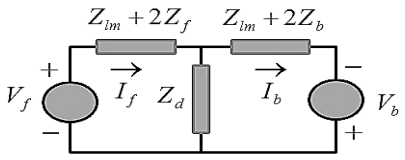

Fig. 2. Equivalent circuit of an ATPIM

It is worth noting that using Eq. (14), the YCIM under an OCFSC will be equivalent to a symmetrical 2-phase IM with n_q turn numbers.

2.2. Voltage RT

According to double revolving field theory, equivalent circuit of an ATPIM can be illustrated as Fig. 2. In Fig. 2 [29]:

$$V_f = 0.5\left(V_m - j\frac{V_a}{k}\right) \tag{15}$$

$$V_b = 0.5\left(V_m + j\frac{V_a}{k}\right) \tag{16}$$

$$I_f = 0.5\left(I_m - jkI_a\right) \tag{17}$$

$$I_b = 0.5\left(I_m + jkI_a\right) \tag{18}$$

Using the following substituting:

$$1 \to \sin\theta_e \tag{19a}$$

$$j \to \cos\theta_e \tag{19b}$$

$$k \to \frac{l_d}{l_q} \tag{19c}$$

$$jV_f \to 0.5V_{qs} \tag{19d}$$

$$V_f \to 0.5V_{ds} \tag{19e}$$

$$V_a \to -V_{\alpha s} \tag{19f}$$

$$V_m \to V_{\beta s} \tag{19g}$$

$$jI_f \to 0.5I_{qs} \tag{19h}$$

$$I_f \to 0.5I_{ds} \tag{19i}$$

$$I_a \to -I_{\alpha s} \tag{19j}$$

$$I_m \to I_{\beta s} \tag{19k}$$

Eqns. (15)-(18) are expressed by Eqns. (14) and (20):

$$\begin{bmatrix} V_{ds} \\ V_{qs} \end{bmatrix} = \left[T_V\right]\begin{bmatrix} V_{\alpha s} \\ V_{\beta s} \end{bmatrix} = \begin{bmatrix} \frac{l_q}{l_d}\cos\theta_e & \sin\theta_e \\ -\frac{l_q}{l_d}\sin\theta_e & \cos\theta_e \end{bmatrix}\begin{bmatrix} V_{\alpha s} \\ V_{\beta s} \end{bmatrix} \tag{20}$$

It is expected that using Eqns. (14) and (20), the faulty machine stator voltage equations are achieved as two sets of coupled equations which have balanced structures. Therefore, the FOC of the faulty YCIM drive can be performed with minor changes in the typical VC scheme.

2.3. VC equations

Equations (21)-(31) are achieved by applying Eqns. (14) and (20) to the faulty YCIM equations (see Appendix).

$$\Omega_e = \Omega_r + \frac{I_{qs}}{T_r I_{ds}} \tag{21}$$

$$\left|\Lambda_r\right| = l_q I_{ds} \tag{22}$$

$$T_e = n_p \frac{l_q}{l_r}\left|\Lambda_r\right| I_{qs} \tag{23}$$

$$V_{ds} = V_{ds}^d + V_{ds}^* + V_{ds}^{ex} \tag{24}$$

$$V_{qs} = V_{qs}^d + V_{qs}^* + V_{qs}^{ex} \tag{25}$$

$$V_{ds}^d = \frac{l_q}{l_r}\left(\frac{l_q I_{ds} - \left|\Lambda_r\right|}{T_r}\right) - \Omega_e I_{qs}\left(l_{qs} - \frac{l_q^2}{l_r}\right) + \left(r_s - \frac{\left(-\frac{l_q^2}{l_d^2}r_s + r_s\right)\left(l_{qs} - \frac{l_q^2}{l_r}\right)}{-\frac{l_q^2}{l_d^2}l_{ds} + l_{qs}}\right) I_{ds} \tag{26}$$

$$V_{ds}^d = \Omega_e I_{ds}\left(l_{qs} - \frac{l_q^2}{l_r}\right) + \Omega_e l_q \frac{\left|\Lambda_r\right|}{l_r}\left(\frac{l_q^2}{l_d^2}r_s - \frac{\left(-\frac{l_q^2}{l_d^2}r_s + r_s\right)\left(\frac{l_q^2}{l_d^2}l_{qs} - \frac{l_q^2}{l_r}\right)}{-\frac{l_q^2}{l_d^2}l_{ds} + l_{qs}}\right) I_{qs} \tag{27}$$

$$\begin{bmatrix} V_{ds}^* \\ V_{qs}^* \end{bmatrix} = \left[K\right]\begin{bmatrix} \left(-\frac{l_q^2}{l_d^2}r_s + r_s\right) I_{ds} + \left(-\frac{l_q^2}{l_d^2}l_{ds} + l_{qs}\right) pI_{ds} \\ \left(-\frac{l_q^2}{l_d^2}r_s + r_s\right) I_{qs} + \left(-\frac{l_q^2}{l_d^2}l_{ds} + l_{qs}\right) pI_{qs} \end{bmatrix} \tag{28}$$

$$\left[K\right] = \begin{bmatrix} -\cos^2\theta_e + \frac{l_{qs} - \frac{l_q^2}{l_r}}{-\frac{l_q^2}{l_d^2}l_{ds} + l_{qs}} & 0.5\sin 2\theta_e \\ 0.5\sin 2\theta_e & \cos^2\theta_e + \frac{\frac{l_q^2}{l_d^2}l_{qs} - \frac{l_q^2}{l_r}}{-\frac{l_q^2}{l_d^2}l_{ds} + l_{qs}} \end{bmatrix} \tag{29}$$

$$V_{ds}^{ex} = \Omega_e\left(\frac{l_q^2}{l_d^2}l_{ds} + l_{qs}\right)\begin{pmatrix} 0.5I_{ds}\sin 2\theta_e \\ -I_{qs}\cos^2\theta_e \end{pmatrix} \tag{30}$$

$$V_{qs}^{ex} = \Omega_e\left(\frac{l_q^2}{l_d^2}l_{ds} + l_{qs}\right)\begin{pmatrix} -0.5I_{qs}\sin 2\theta_e \\ +I_{ds}\sin^2\theta_e \end{pmatrix} \tag{31}$$

2.4. Inverter configuration

One of the key subjects for the post-fault operation of YCIM drive systems against an OCFSC is the inverter

configuration. After the OCFSC, various inverter configurations can be utilized to drive the faulty YCIM. For example, 3-leg inverter configuration with connection of the neutral point to the middle-point of the inverter DC-link, 3-leg inverter with connection of the neutral point to the faulty phase, four-leg inverter with connection of the faulty phase to an extra leg, etc. [30, 31]. The present study employs the same inverter configuration as used in Refs. [5, 6] because of simple structure and low price. Fig. 3 shows the schematic diagram of the used inverter configuration in this paper to drive the YCIM against an OCFSC.

Regarding the used YCIM in this paper, the maximum allowed load for the faulty YCIM drive is 1/3 of the nominal torque [6]. It is worth noting that, in this study an overall VC method for YCIM drives under an OCFSC, appropriate for all categories of inverter configurations is presented.

2.5. Proposed VC scheme

VC emerged after scalar control strategies in order to provide better performances. Different VC approaches for IMs have been developed in the past years. The indirect VC strategy based on the orientation of the rotor flux is a well-known system in order to achieve an effective control for IM drive systems [32, 33].

As can be seen from Eqns. (21)-(31), the faulty machine equations are achieved as the healthy machine equations. Consequently it is possible to control the YCIM under an OCFSC with some changes in the typical VC scheme. The schematic diagram of the typical indirect VC method based on the rotor flux is shown in Fig. 4. Based on this figure and Eqns. (21)-(31), the proposed VC scheme for YCIM drives under an OCFSC is illustrated in Fig. 5.

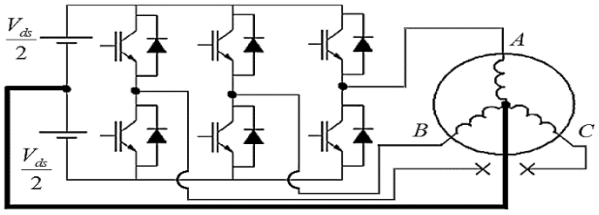

Fig. 3. Schematic diagram of the inverter configuration to drive the YCIM against an OCFSC

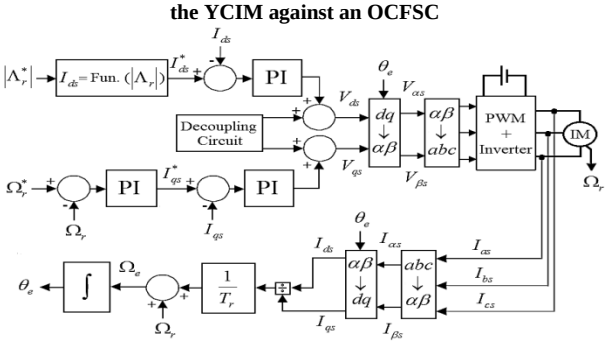

Fig. 4. Schematic diagram of the typical indirect VC method

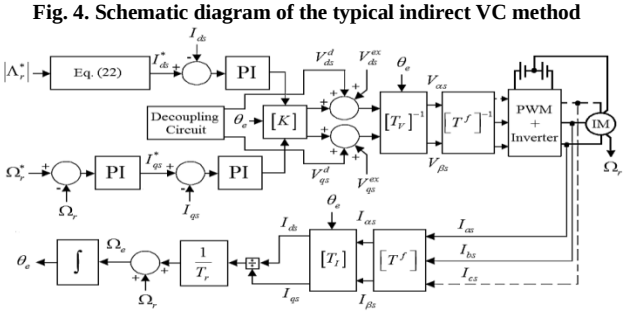

Fig. 5. Schematic diagram of the proposed VC scheme for YCIM drives under an OCFSC

In Fig. 5 [13]:

$$\left[T^{f}\right]=\sqrt{2}\begin{bmatrix}0.5 & -0.5\\ 0.5 & 0.5\end{bmatrix} \tag{32}$$

In the proposed scheme of Fig. 5, the reference rotor flux and the error between the reference and real values of the speed with the speed PI controller are used to determine the reference currents. The error between the reference and real currents using PI controllers and matrix $[K]$ determines the reference voltages. As shown, the dq motor voltages are achieved from the reference voltages, decoupling circuit voltages and two extra voltages. The motor voltages in the ab frame are the inputs of the PWM. The generated signals from the PWM are the inputs of the voltage source inverter. In Fig. 5, the rotor flux position is obtained based on the currents, speed, and motor parameters.

3. GENETIC ALGORITHM

PI controllers are very common in VC strategies to acquire the control variables. These controllers have simple structure and low cost. Nevertheless, the problem in implementation of PI controller is to set the optimum parameters of PI controllers [16].

Recently, there has been increasing interest and development in the field of evolutionary algorithms. Genetic algorithm has widespread applications in control system optimization difficulties. Genetic algorithm is an adaptive search strategy that mimics the evolution process based on the Darwin's survival of the fittest method. Compared to other optimization techniques, genetic algorithm is particularly effective at avoiding local minima, which can be a specific feature of nonlinear systems [34, 35]. As shown in the proposed improved VC method, three PI controllers are used. The regulation of the parameters of PI controllers has a significant effect in the precision of the proposed approach. In this work, the genetic algorithm is utilized to determine the optimal parameters for PI controller blocks. The optimization process using genetic

algorithm is summarized in Fig. 6 [36].

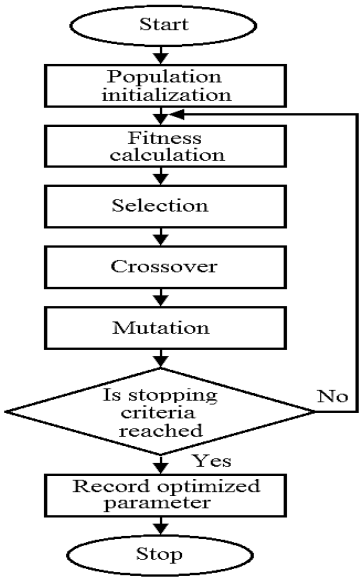

Fig. 6. Optimization steps using genetic algorithm

The optimization processes are given as:

- Initialization of population
- Evaluation of fitness
- Selection of individual
- Crossover
- Mutation

One of the most important steps in genetic algorithm is to select the fitness function. In this paper, the fitness function is achieved from the Integral of the Square Error (ISE) as Eq. (33) [37]:

$$F_i = \int_0^{\infty} \left(\Omega_r^* - \Omega_r\right)^2 dt \tag{33}$$

Roulette wheel is used for choosing desired individual. Probability of selection for individual *i* [38]:

$$p_i = \frac{F_i}{\sum_{i=1}^{N} F_i} \tag{34}$$

Parameters used in genetic algorithm for optimization of PI controllers are as:

- Number of generation=50
- Population size=30
- Crossover probability=[0 1]
- Mutation probability=0.6

In this paper, an offline tuning method using genetic algorithm is utilized for tuning PI parameters since it needs several iterations. The procedure includes two steps. At first a time response simulation is performed in the computer. Then, the optimal parameters for the PI controllers are passed to the real time controller. The optimized parameters for the PI controllers are summarized in Table 1.

Table 1. Optimal parameters for the PI controllers

Speed controller	$K_p^S = 0.4$, $K_i^S = 3$
Current controllers	$K_p^i = 230$, $K_i^i = 8$

Table 2. YCIM specifications

Nominal power	0.75kW
Nominal torque	5.7N.m
Frequency	50Hz
Mutual inductance	0.6H
Stator and rotor self-inductances	0.61H
Rotor resistance	14.64Ω
Stator resistance	10.44Ω
Moment of inertia	0.016kg.m^2
Number of poles	2

Fig. 7. Experimental setup

4. EXPERIMENTAL RESULTS

To confirm the system performance with the proposed improved VC strategy, several tests have been carried out. The experimental setup is displayed in Fig. 7.

In tests, the YCIM with the neutral point accessibility and a DC machine driven by a resistivity bank are employed. The typical VC strategy based on Fig. 4, the presented VC method in Ref. [16], and the developed VC strategy in this paper based on Fig. 5 with and without genetic algorithm for the YCIM are programmed using PSIM software and implemented using DSP/TMS320F28335 microcontroller. The sampling time of VC systems is fixed to 100μs and OCFSC happens in phase *c*. In all tests, the neutral point is connected to the middle-point of the inverter DC-link, $\left|\Lambda_r^*\right| = 1\text{wb}$, and the rotor flux signal is obtained based on stator d-axis current ($\left|\Lambda_r\right| = l_q I_{ds}$). Table 2 shows the YCIM specifications.

In experiments, the typical VC method and the proposed control strategy with optimized PI controllers are compared as the first scenario. Then, the introduced FOC method without optimized PI controllers and the introduced FOC method with optimized PI controllers are compared (second scenario). Finally, the presented VC method in Ref. [16] and the proposed improved VC method with optimized PI controllers are compared (third scenario).

4.1. First scenario

Fig. 8 shows the transient and steady-state performances using the proposed improved VC technique with the genetic algorithm and the typical VC method after the OCFSC. In Fig. 8, a step change in the machine speed is considered, where the reference speed is changed from 100rad/s to 60rad/s. Fig. 8 displays the behaviors of the speed, rotor flux, electromagnetic torque, and phase currents. As shown, using the proposed improved VC approach, the speed, rotor flux, and torque ripples are eliminated for the faulty YCIM drive. According to the experimental results of Fig. 8(a), suitable tracking performances of the motor speed and flux are achieved during the post-fault situation. In addition, the torque of the faulty YCIM has good performances during different speeds and it changes in terms of the speed change. It is also observed that the healthy phases of the faulty YCIM can be controlled separately and they are perfectly balanced and sinusoidal compared to the typical VC method. To sum up, steady-state speed, rotor flux, and torque ripples at speed of 100rad/s as well as dynamic response for Fig. 8 are compared in Table 3.

Table 3. Comparison of the steady-state speed, rotor flux, and torque ripples as well as the dynamic response for Fig. 8

Items \ Methods	Proposed improved FOC technique with the genetic algorithm	Typical FOC method
Speed ripples (rad/s)	1.9	4.8
Rotor flux ripples (wb)	0.034	0.07
Torque ripples (N.m)	0.25	0.65
Dynamic response (s)	0.26	0.42

Table 4. Comparison of the steady-state speed, rotor flux, and torque ripples as well as the dynamic response for Fig. 9

Items \ Methods	Proposed improved FOC technique with the genetic algorithm	Proposed improved FOC technique without the genetic algorithm
Speed ripples (rad/s)	1.6	2.8
Rotor flux ripples (wb)	0.028	0.047
Torque ripples (N.m)	0.2	0.33
Dynamic response (s)	0.38	0.59

Table 5. Comparison of the steady-state speed, rotor flux, and torque ripples for Fig. 10.

Items \ Methods	Proposed improved FOC technique with the genetic algorithm	Presented FOC technique in Ref. [16]
Speed ripples (rad/s)	2.2	3.6
Rotor flux ripples (wb)	0.039	0.068
Torque ripples (N.m)	0.44	0.64

4.2. Second scenario

Fig. 9 shows the transient and steady-state performances using the proposed improved VC technique with and without genetic algorithm after the OCFSC. Fig. 9(a) shows the performance of the proposed improved VC technique with genetic algorithm and Fig. 9(b) shows the performance of the proposed improved VC technique without genetic algorithm. In Fig. 9, a step change in the YCIM speed is considered, where the reference speed is changed from 70rad/s to 110rad/s. Fig. 9 displays the behaviors of the speed, rotor flux, and electromagnetic torque. It can be observed that the proposed improved VC strategy provides better performances in speed, rotor flux, and electromagnetic torque responses during the transient and steady-state when the optimized values of the parameters of PI controllers are used. It is also seen that the healthy phases of the faulty YCIM using the proposed improved FOC technique with genetic algorithm are more sinusoidal compared to those of the proposed improved FOC technique without genetic algorithm. To sum up, the steady-state speed, rotor flux, and torque ripples at the speed of 70rad/s as well as the dynamic response for Fig. 9 are compared in Table 4.

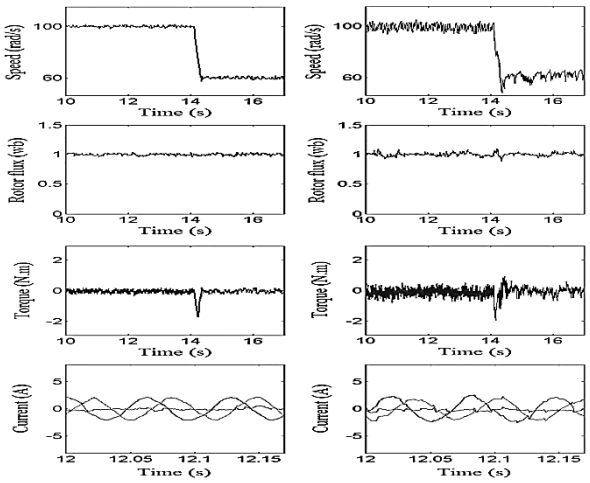

(a) (b)

Fig. 8. Experimental results of the proposed improved FOC technique with the genetic algorithm and the typical FOC method after the OCFSC; (a) proposed improved FOC technique with the genetic algorithm, (b) typical FOC method

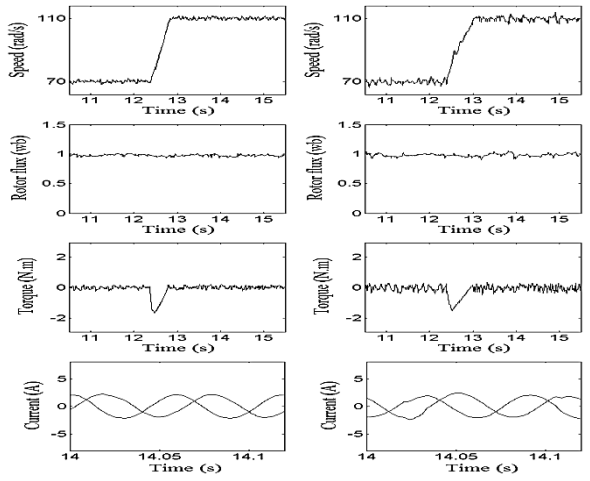

(a) (b)

Fig. 9. Experimental results of the proposed improved FOC technique with and without genetic algorithm after the OCFSC; (a) with genetic algorithm, (b) without genetic algorithm

Table 6. Comparison of different FOC strategies under an OCFSC

Methods / Items	Presented method in Ref. [5]	Presented method in Ref. [16]	Presented method in Ref. [14]	Presented method in Ref. [13]	Presented method in Ref. [6]	Proposed improved FOC method
Control method	Indirect FOC	Indirect FOC	Direct FOC	Direct FOC	Indirect FOC	Indirect FOC
Controller	Current controller	Voltage controller	Voltage controller	Current controller	Voltage controller	Voltage controller
Speed, flux, and torque ripples (accuracy)	Medium (medium)	Low (high)	Low (high)	Medium (medium)	Very low (very high)	Very low (very high)
Complexity	Low	Medium	Very high	Medium	Very high	Medium

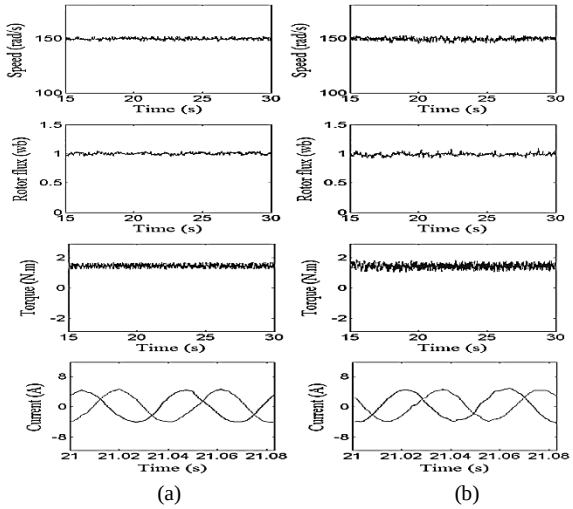

(a) (b)

Fig. 10. Experimental results of the proposed improved FOC method and the presented FOC technique in Ref. [16] after the OCFSC; (a) proposed improved FOC method, (b) presented FOC technique in Ref. [16].

4.3. Third scenario

The performances of the proposed improved VC method and the presented VC technique in Ref. [16] during the post-fault operation are analyzed in this scenario. The results obtained are displayed in Fig. 10. In Fig. 10(a), the parameters of PI controllers are tuned using the genetic algorithm and in Fig. 10(b), the parameters of PI controllers are optimized using the particle swarm optimization algorithm. In Fig. 10 the reference speed is maintained at 150rad/s. Fig. 10 displays the performances of the motor speed, rotor flux, and electromagnetic torque. In both tests, a load torque equal to 1.5N.m (around 80% of the maximum achievable post-fault load torque) is considered.

As shown, the tracking performance of the YCIM speed and YCIM rotor flux are quite accurate even after the load in both tests. It can be seen that the proposed improved VC strategy in this study provides lower speed, rotor flux, and electromagnetic torque ripples compared to the presented VC technique in Ref. [16]. The results indicate that the speed, rotor flux, and electromagnetic torque ripples of the faulty YCIM decrease when the leakage inductance is considered in the VC equations. To sum up, the steady-state speed, rotor flux, and torque ripples for Fig. 10 are compared in Table 5.

5. COMPARISON AND DISCUSSION

Based on the experimental results, the proposed improved FOC strategy after the OCFSC is more accurate than the typical FOC method and the presented FOC technique in Ref. [16]. It is worth noting that the proposed improved FOC method in this paper has high accuracy like the presented FOC technique in Ref. [6]. However, the proposed scheme uses fewer PI controllers compared to Ref. [6]. To sum up, Table 6 represents the comparison of different FOC strategies under an OCFSC.

6. CONCLUSION

In this paper, an improved VC system with the genetic algorithm is designed and its performance is confirmed against an OCFSC. The proposed improved VC approach is based on using two different RTs. In the proposed modified controller, the genetic algorithm is employed for tuning of PI controllers. The performance of the introduced control technique is experimentally validated in a 0.75kW YCIM drive considering an OCFSC. Provided experiments analyze the steady-state and transient performances during different speeds. Based on the experimental results, although the typical VC can control the faulty YCIM, it has very poor dynamic and steady-state responses. In addition, the proposed improved VC with the genetic algorithm has better performances compared to the proposed improved VC without genetic algorithm. In contrast with the presented VC method in Ref. [16], the proposed controller provides low speed, rotor flux, and torque ripples.

APPENDIX

Equations (A1)-(A12) are achieved by applying Eqns. (14) and (20) to the faulty YCIM equations.

Stator voltage equations:

$$\begin{aligned}&\left[T_V\right]\begin{bmatrix}V_{\alpha s}\\V_{\beta s}\end{bmatrix}=\\&\left[T_V\right]\begin{bmatrix}r_s+l_{ds}p & 0\\0 & r_s+l_{qs}p\end{bmatrix}\left[T_I\right]^{-1}\left[T_I\right]\begin{bmatrix}I_{\alpha s}\\I_{\beta s}\end{bmatrix}\\&+\left[T_V\right]\begin{bmatrix}l_d p & 0\\0 & l_q p\end{bmatrix}\left[T\right]^{-1}\left[T\right]\begin{bmatrix}I_{\alpha r}\\I_{\beta r}\end{bmatrix}\end{aligned}\qquad \text{(A1)}$$

where,

$$[T]=\begin{bmatrix}\cos\theta_e & \sin\theta_e\\ -\sin\theta_e & \cos\theta_e\end{bmatrix} \quad (A2)$$

Equation (A1) is simplified as Eqns. (A3) and (A4):

$$V_{ds}=r_s I_{ds}+l_{qs}pI_{ds}-\Omega_e l_{qs}I_{qs}+l_q pI_{dr}-\Omega_e l_q I_{qr}$$
$$+\left(\frac{l_q^2}{l_d^2}r_s-r_s\right)\left(I_{ds}\cos^2\theta_e-0.5I_{qs}\sin 2\zeta_e\right)+ \quad (A3)$$
$$\left(\frac{l_q^2}{l_d^2}l_{ds}-l_{qs}\right)\begin{pmatrix}-I_{ds}\sin 2\theta_e+pI_{ds}\cos^2\theta_e-\\ I_{qs}\cos 2\theta_e-0.5pI_{qs}\sin 2\theta_e+\\ 0.5\Omega_e I_{ds}\sin 2\theta_e-\Omega_e I_{qs}\sin^2\theta_e\end{pmatrix}$$

$$V_{qs}=r_s I_{qs}+l_{qs}pI_{qs}+\Omega_e l_{qs}I_{ds}+\Omega_e l_q I_{dr}+l_q pI_{qr}$$
$$+\left(\frac{l_q^2}{l_d^2}r_s-r_s\right)\left(-0.5I_{ds}\sin 2\theta_e+I_{qs}\sin^2\theta_e\right)+ \quad (A4)$$
$$\left(\frac{l_q^2}{l_d^2}l_{ds}-l_{qs}\right)\begin{pmatrix}-I_{ds}\cos 2\theta_e-0.5pI_{ds}\sin 2\theta_e\\ +I_{qs}\sin 2\theta_e+pI_{qs}\sin^2\theta_e+\\ \Omega_e I_{ds}\cos^2\theta_e-0.5\Omega_e I_{qs}\sin 2\theta_e\end{pmatrix}$$

Rotor voltage equations:

$$[T]\begin{bmatrix}V_{\alpha r}\\ V_{\beta r}\end{bmatrix}=[T]\begin{bmatrix}r_r+l_r p & \Omega_r L_r\\ -\Omega_r L_r & r_r+l_r p\end{bmatrix}[T]^{-1}[T]\begin{bmatrix}I_{\alpha r}\\ I_{\beta r}\end{bmatrix}$$
$$+[T]\begin{bmatrix}l_d p & \Omega_r l_q\\ -\Omega_r l_d & l_q p\end{bmatrix}[T_I]^{-1}[T_I]\begin{bmatrix}I_{\alpha s}\\ I_{\beta s}\end{bmatrix} \quad (A5)$$

Equation (A5) is simplified as Eqns. (A6) and (A7):

$$V_{dr}=r_r I_{dr}+l_r pI_{dr}-(\Omega_e-\Omega_r)l_r I_{qr}$$
$$+l_q pI_{ds}-(\Omega_e-\Omega_r)l_q I_{qs} \quad (A6)$$

$$V_{qr}=r_r+l_r pI_{qr}+(\Omega_e-\Omega_r)l_r I_{dr}$$
$$+l_q pI_{qs}+(\Omega_e-\Omega_r)l_q I_{ds} \quad (A7)$$

Rotor flux equations:

$$[T]\begin{bmatrix}\Lambda_{\alpha r}\\ \Lambda_{\beta r}\end{bmatrix}=[T]\begin{bmatrix}l_d & 0\\ 0 & l_q\end{bmatrix}[T_I]^{-1}[T_I]\begin{bmatrix}I_{\alpha s}\\ I_{\beta s}\end{bmatrix}$$
$$+[T]\begin{bmatrix}l_r & 0\\ 0 & l_r\end{bmatrix}[T]^{-1}[T]\begin{bmatrix}I_{\alpha r}\\ I_{\beta r}\end{bmatrix} \quad (A8)$$

Equation (A8) is simplified as Eqns. (A9) and (A10):

$$\Lambda_{dr}=l_q I_{ds}+l_r I_{dr} \quad (A9)$$

$$\Lambda_{qr}=l_q I_{qs}+l_r I_{qr} \quad (A10)$$

Torque equation:

$$T_e=n_p\left(l_q I_{\beta s}I_{\alpha r}-l_d I_{\alpha s}I_{\beta r}\right)=$$
$$n_p\begin{bmatrix}I_{\alpha r} & I_{\beta r}\end{bmatrix}\begin{bmatrix}0 & l_q\\ -l_d & 0\end{bmatrix}\begin{bmatrix}I_{\alpha s}\\ I_{\beta s}\end{bmatrix}= \quad (A11)$$
$$\begin{pmatrix}n_p\left([T]\begin{bmatrix}I_{\alpha r}\\ I_{\beta r}\end{bmatrix}\right)^T\left([T]^{-1}\right)^T\\ \cdot\begin{bmatrix}0 & l_q\\ -l_d & 0\end{bmatrix}[T_I]^{-1}[T_I]\begin{bmatrix}I_{\alpha s}\\ I_{\beta s}\end{bmatrix}\end{pmatrix}$$

Equation (A11) is simplified as Eq. (A12):

$$T_e=n_p l_q\left(I_{qs}I_{dr}-I_{ds}I_{qr}\right) \quad (A12)$$

According to Eqns. (A1)-(A12) and using $\Lambda_{dr}=|\Lambda_r|$, $\Lambda_{qr}=0$ (VC principals), the VC equations of the YCIM under an OCFSC are expressed as Eqns. (21)-(31).

REFERENCES

[1] D. Zhou et al., "An embedded closed-loop fault-tolerant control scheme for nonredundant VSI-fed induction motor drives", *IEEE Trans. Power Electron.*, vol. 32, pp. 3731-40, 2016.

[2] C. Yeh and N. Demerdash, "Fault-tolerant soft starter control of induction motors with reduced transient torque pulsations", *IEEE Trans. Energy Convers.*, vol. 24, pp. 848-59, 2009.

[3] B. Yelamarthi and S. Sandepudi, "Predictive torque control of three-phase induction motor drive with inverter switch fault-tolerance capabilities", *IEEE J. Emerg. Selected Top. Power Electron.*, 2020.

[4] A. Sayed-Ahmed and N. Demerdash, "Fault-tolerant operation of delta-connected scalar-and vector-controlled AC motor drives", *IEEE Trans. Power Electron.*, vol. 27, pp. 3041-9, 2011.

[5] M. Shabandokht-Zarami et al., "A modified FOC strategy with optimal rotor flux for FTC of star-connected TPIMDs against single-phase open fault", *IEEE Canadian J. Electr. Comput. Eng.*, vol. 44, pp. 83-93, 2021.

[6] H. Abbasi et al., "IRFOC of induction motor drives under open-phase fault using balanced and unbalanced transformation matrices", *IEEE Trans. Ind. Electron.*, 2020.

[7] M. Manohar and S. Das, "Current sensor fault-tolerant control for direct torque control of induction motor drive using flux-linkage observer", *IEEE Trans. Ind. Inf.*, vol. 13, pp. 2824-33, 2017.

[8] B. Tabbache et al., "control reconfiguration strategy for post-sensor FTC in induction motor-based EVs", *IEEE Trans. Veh. Tech.*, vol. 62, pp. 965-71, 2012.

[9] Y. Liu, M. Stettenbenz, and A. Bazzi, "Smooth fault-tolerant control of induction motor drives with sensor failures", *IEEE Trans. Power Electron.*, vol. 34, pp. 3544-52, 2018.

[10] D. Kastha and B. Bose, "On-line search based pulsating torque compensation of a fault mode single-phase variable frequency induction motor drive", *IEEE Trans. Ind. Appl.*, vol. 31, pp. 802-11, 1995.

[11] A. Sayed-Ahmed and N. Demerdash, "Control of open-loop PWM delta-connected motor-drive systems under One phase failure condition", *J. Power Electron.*, vol. 11, pp. 824-36, 2011.

[12] A. Sayed-Ahmed, B. Mirafzal, and N. Demerdash, "Fault-tolerant technique for Δ-connected AC-motor drives", *IEEE Trans. Energy Conv.*, vol. 26, pp. 646-53, 2010.

[13] Y. Zhao and T. Lipo, "An approach to modeling and field-oriented control of a three phase induction machine with structural imbalance", *Proc. Appl. Power Electron. Conf.*, USA, 1996.

[14] R. Tabasian et al., "Direct field-oriented control strategy for fault-tolerant control of induction machine drives based on EKF", *IET Electr. Power Appl.*, 2020.

[15] T. Liu, J. Fu, and T. Lipo, "A strategy for improving

reliability of field-oriented controlled induction motor drives", *IEEE Trans. Ind. Appl.*, vol. 29, pp. 910-8, 1993.
[16] M. Nikpayam et al., "An optimized vector control strategy for induction machines during open-phase failure condition using particle swarm optimization algorithm", *Int. Trans. Electr. Energy Syst.*, vol. 30, 2020.
[17] M. Jannati et al., "Experimental evaluation of FOC of 3-phase IM under open-phase fault", *Int. J. Electron.*, vol. 104, pp. 1675-88, 2017.
[18] M. Jannati, N. Idris, and M. Aziz, "Performance evaluation of the field-oriented control of star-connected 3-phase induction motor drives under stator winding open-circuit faults", *J. Power Electron.*, vol. 16, pp. 982-93, 2016.
[19] M. Jannati and N. Idris, "Vector control of unbalanced 3-phase IM using forward and backward components", *Turkish J. Electr. Eng. Comput. Sci.*, vol. 25, pp. 1358-74, 2017.
[20] T. Banerjee et al., "Off-line optimization of PI and PID controller for a vector controlled induction motor drive using PSO", *Proc. Int. Conf. Electr. Comput. Eng.*, Bangladesh, 2010.
[21] M. Hannan et al., "Quantum-behaved lightning search algorithm to improve indirect field-oriented Fuzzy-PI control for IM drive", *IEEE Trans. Ind. Appl.*, vol. 54, pp. 3793-805, 2018.
[22] T. Orlowska-Kowalska and K. Szabat, "Optimization of fuzzy-logic speed controller for DC drive system with elastic joints", *IEEE Trans. Ind. Appl.*, vol. 40, pp. 1138-44, 2004.
[23] S. Sebtahmadi et al., "A PSO-DQ current control scheme for performance enhancement of Z-source matrix converter to drive IM fed by abnormal voltage", *IEEE Trans. Power Electron.*, vol. 33, pp. 1666-81, 2017.
[24] R. Selvi and R. Malar, "A bridgeless Luo converter based speed control of switched reluctance motor using Particle Swarm Optimization (PSO) tuned proportional integral (Pi) controller", *Microproc. Microsyst.*, vol. 75, 2020.
[25] D. Corus and P. Oliveto, "Standard steady state genetic algorithms can hillclimb faster than mutation-only evolutionary algorithms", *IEEE Trans. Evol. Comput.*, vol. 22, pp. 720-32, 2017.
[26] A. Jafari et al., "Hybrid optimization technique using exchange market and genetic algorithms", *IEEE Access*, vol. 8, pp. 2417-27, 2019.
[27] K. Lee et al., "Moving least square-based hybrid genetic algorithm for optimal design of w-band dual-reflector antenna", *IEEE Trans. Magnetics*, vol. 55, pp. 1-4, 2019.
[28] D. Pradhan et al., "CBGA-ES+: a cluster-based genetic algorithm with non-dominated elitist selection for supporting multi-objective test optimization", *IEEE Trans. Soft. Eng.*, 2011.
[29] M. Jannati, N. R. Idris, and Z. Salam, "A new method for modeling and vector control of unbalanced induction motors", *Energy Con. Congress Expos.*, USA, 2012.
[30] R. Tabasian et al., "Control of three-phase induction machine drives during open-circuit fault: A review", *IETE J. Res.*, vol. 18, pp. 1-8, 2020.
[31] M. Tousizadeh et al., "Performance comparison of fault-tolerant three-phase induction motor drives considering current and voltage limits", *IEEE Trans. Ind. Electron.*, vol. 66, pp. 2639-48, 2018.
[32] J. Jain, S. Ghosh, and S. Maity, "A numerical bifurcation analysis of indirect vector-controlled induction motor", *IEEE Trans. Control Syst. Tech.*, vol. 26, pp. 282-90, 2017.
[33] K. Wang et al., "An improved indirect field-oriented control scheme for linear induction motor traction drives", *IEEE Trans. Ind. Electron.*, vol. 65, pp. 9928-37, 2018.
[34] W. da Silva, P. Acarnley, and J. Finch, "Application of genetic algorithms to the online tuning of electric drive speed controllers", *IEEE Trans. Ind. Electron.*, vol. 47, pp. 217-19, 2000.
[35] F. Lin, P. Huang, and W. Chou, "Recurrent-fuzzy-neural-network-controlled linear induction motor servo drive using genetic algorithms", *IEEE Trans. Ind. Electron.*, vol. 54, pp. 1449-61, 2007.
[36] G. Demir and R. Vural, "Speed control method using genetic algorithm for permanent magnet synchronous motors", *Proc. 6th Int. Conf. Control Eng. Inf. Tech.*, Turkey, 2018.
[37] P. Rensburg, I. Shaw, and J. Wyk, "Adaptive PID control using a genetic algorithm", *Proc. Sec. Int. Conf. Knowledge-Based Intell. Electron. Syst.*, Australia, 1998.
[38] F. Pan, R. Han, and R. Zhang, "An optimal controller based-on GA for direct torque control", *Proc. Third Int. Conf. Genetic Evol. Comput.*, China, 2009.